Published in final edited form as:
J Microencapsul. 2011 ; 28(5): 344–352. doi:10.3109/02652048.2011.569764.

Phase-separated chitosan–fibrin microbeads for cell delivery

Zhewei Chen, **Limin Wang**, and **Jan P. Stegemann**
Department of Biomedical Engineering, University of Michigan, Ann Arbor MI, USA

Abstract

Matrix-enhanced delivery of cells is a promising approach to improving current cell therapies. Our objective was to create cell-laden composite microbeads that combine the attractive features of the natural polymers chitosan and fibrin. Liquid polydimethylsiloxane was used to emulsify a chitosan–fibrinogen solution containing suspended human fibroblast cells, followed by initiation of thrombin-mediated polymerization of fibrin and thermal/pH-mediated gelation of chitosan. Chitosan/fibrin weight percent (wt%) ratios of 100/0, 75/25, 50/50 and 25/75 were investigated. Microbead diameters ranged from 275 ± 99 μm to 38 ± 10 μm using impeller speeds from 600 to 1400 rpm. Fibroblasts remained viable on day 1 post-fabrication in all matrices, but cell viability was markedly higher in high-fibrin microbeads by day 8 post-fabrication. Cell spreading and interaction with the extracellular matrix was also markedly increased in high-fibrin matrices. Such composite microbeads containing viable entrapped cells have potential for minimally invasive delivery of cells for a variety of tissue repair applications.

Keywords

Microsphere; cell therapy; tissue engineering; regenerative medicine; matrix

Introduction

A main goal of cell-based therapies is to deliver cells to a site of disease or injury in order to augment or replace the function of the damaged tissue (Lee et al., 2009; Chavakis et al., 2010). For this approach to be successful, it is necessary that the transplanted cells stay in the desired location, remain viable and also that they perform the desired tissue-specific functions. A variety of approaches to achieving these goals are currently being developed. In particular, the creation of tissue “modules” that mimic the environment of a 3D tissue has been proposed as a way to deliver cells in a minimally invasive manner, while also promoting desired cell phenotypes and subsequent self-assembly of modules into larger tissue structures (McGuigan et al., 2008; Nichol and Khademhosseini, 2009; Livoti and Morgan, 2010). An example of this approach is the creation of “microbeads” consisting of biological macromolecules surrounding encapsulated cells (Batorsky et al., 2005; Chan et al., 2010). By using naturally derived materials as the microbead matrix, cell compatibility is enhanced and the composition of the matrix can be designed to promote cell adhesion, proliferation and/or differentiation (Lund et al., 2008, 2009).

Address for correspondence: Jan P. Stegemann, Department of Biomedical Engineering, University of Michigan, 1101 Beal Avenue, Ann Arbor, MI 48109, USA. Tel: +734-764-8313. Fax: +734-647-4834. jpsteg@umich.edu.

Declaration of interest
The authors report no declarations of interest.

Biomacromolecule-based microbeads have been fabricated using water-in-oil emulsion systems (Gorodetsky et al., 1999; Batorsky et al., 2005) droplet generation (Perka et al., 2001; Mark et al., 2009) and by microfluidics (Choi et al., 2007; Breslauer et al., 2010). In most cases such microspheres are made in the absence of cells, for use as drug or growth factor delivery vehicles (Addo et al., 2010; Solorio et al., 2010) or as microcarrier substrates for subsequent attachment of cells to the surface (Gorodetsky et al., 2004; Natesan et al., 2010). In some cases, cells have been entrapped directly inside the microbeads. For example, alginate and agarose (both long-chain polysaccharides derived from seaweed) have been used for this purpose (Sakai et al., 2005; Mazumder et al., 2009). However, mammalian cells do not have receptors for attachment to these polysaccharide materials, and therefore embedded cells do not receive biological cues from the surrounding insoluble matrix. For this reason, other materials, as well as blends of materials, have been used in order to enhance cell–matrix interactions with microbeads (Lund et al., 2008; Maeng et al., 2010; Yu et al., 2010).

Chitosan is an N-acetyl-polysaccharide derived from chitin, the structural polymer in arthropod exoskeletons (Kurita, 2006). It has been used in a variety of biomedical applications because it contains amino groups that can be used to functionalize the molecule, and which increase compatibility with other proteins and cells (Berger et al., 2004; Jiang et al., 2008). Chitosan also exhibits robust mechanical properties (Yamaguchi et al., 2003) and therefore has been used widely as a scaffold material in tissue engineering (Madihally and Matthew, 1999; Costa-Pinto et al., 2009). In most current applications, chitosan scaffolds are pre-fabricated, dehydrated and subsequently seeded with cells. However, it is also possible to create chitosan hydrogels by dissolving the macromolecule in weak acid, which causes its amino groups to become cationic (Lavertu et al., 2008). The addition of the weak base glycerol-2-phosphate (β-GP) and subsequent elevation of the temperature causes a sol–gel transition and reconstitution of the chitosan polymer. Such methods have been used to encapsulate cells in a chitosan matrix under conditions which maintain cell viability and function (Nair et al., 2007; Wang and Stegemann, 2010).

Fibrin is a clotting protein derived from the blood plasma protein fibrinogen. It is integral to the wound healing process (Mosesson, 2005; Laurens et al., 2006), and therefore is an intensively studied protein that has found utility in tissue engineering and regenerative medicine (Breen et al., 2009). Fibrin hydrogel formation is initiated by cleavage of specific fibrinopeptide sequences from the larger fibrinogen molecule by the enzyme thrombin. The resulting fibrin monomers rapidly self-assemble to form entangled networks of fibrin fibers. Such 3D fibrin networks have been used as scaffold materials in tissue engineering (Ahmed et al., 2008) and for cell delivery (Gurevich et al., 2002), because of the ability of fibrin to support cell adhesion, growth and differentiated function (Hong and Stegemann, 2008). Fibrin matrices tend to be highly compliant and extensible, and can be degraded by the enzyme plasmin, which is produced by a variety of cell types. However, the low mechanical properties of fibrin have posed a challenge in creating robust cellular scaffolds using this material alone (Cummings et al., 2004).

Our goal in this study was to combine the attractive structural and biochemical features of the polysaccharide chitosan and the protein fibrin to create modular microbeads for use in cell delivery and tissue regeneration. Importantly, our intent was to embed cells directly in the chitosan–fibrin matrix at the time of microbead fabrication. This necessitated that a cell-friendly process be developed, in which cell viability could be maintained while still creating robust and functional microbeads. This article reports on the method we developed and shows initial characterization of the cellular component. Fibroblast cells were chosen in this study to provide a proof of concept, however the method can be directly extended to other cell types that have specific therapeutic potential. Matrix-enhanced cell delivery in

modular 3D microtissues is an attractive approach in many tissue regeneration applications, since the matrix can be tailored to promote tissue-specific functions, and because delivery in an extracellular matrix may enhance retention and engraftment of cells at the desired site of action.

Materials and methods

Preparation of solutions

Bovine fibrinogen (Sigma Chemical Co., St. Louis, MO) was dissolved in phosphate buffered saline (PBS) to obtain a 60.0 mg/mL fibrinogen stock solution. Bovine thrombin (Sigma) was dissolved in PBS to obtain a 5.0 U/mL thrombin stock solution. β-GP was dissolved in deionized water to obtain a 58 wt.% β-GP stock solution. Chitosan (93% DDA; BioSyntech, Quebec, Canada) was dissolved in 0.1 N acetic acid (Sigma) to obtain a 2.0 wt. % chitosan stock solution. This solution was autoclaved at 120°C for 20 min to ensure solution sterility. Fibrinogen, thrombin and β-GP stock solutions were sterile filtered. All solutions were kept refrigerated at 4°C before use.

Microbead fabrication

The process used to create chitosan–fibrin microbeads is shown schematically in Figure 1. A chitosan–β-GP solution was created by adding 0.2 mL of β-GP stock solution drop-wise into 0.5 mL of chitosan stock solution under vortexing. To this mixture was added 0.5 mL of fibrinogen stock solution at the appropriate concentration to obtain the desired chitosan/fibrinogen mass ratio (100/0, 75/25, 50/50 or 25/75), as well as 0.1 mL of thrombin stock solution to initiate fibrin formation. All solutions were kept cool at ~4°C during mixing to keep chitosan–β-GP mixtures in a liquid state. The final matrix solution volume was therefore 1.3 mL. In all formulations, the concentration of chitosan was 7.7 mg/mL, the concentration of β-GP was 89.2 mg/mL and the concentration of thrombin was 0.39 U/mL. As shown in Table 1, the fibrinogen content of microbead formulations was progressively increased to produce microbeads differing ratios of chitosan to fibrin (CHI/FIB), as follows: 0 wt.% (100/0), 25 wt.% (75/25), 50 wt.% (50/50) and 75 wt.% (25/75). Pure fibrin microbeads were too fragile for handling, and therefore were not included in this study.

The liquid matrix mixture was injected at a rate of 2.0 mL/min into 80 mL of liquid polydimethylsiloxane (PDMS; SilTech, Miamisburg, OH) under constant stirring using a mixing apparatus (Barnant Co., Barrington, IL) with a custom double-bladed impeller. Emulsification was carried out at the desired impeller speed ("Quantification of microbead size" section) for 10 min while the PDMS was maintained cold in a crushed ice bath. Once the liquid matrix droplets were fully emulsified, the PDMS bath was transferred to a water bath at 37°C for 20 min with constant stirring to simultaneously initiate thermal gelation of the chitosan as well as enzymatic gelling of the fibrin matrix. After microbead gelling, the emulsification vessel was again surrounded with crushed ice and the beads were allowed to stabilize for 10 min with stirring at 450 rpm.

To collect the formed microbeads, the contents of the emulsification vessel were mixed with an equal volume of PBS containing 100 ppm of polypropylene oxide–polyethylene oxide surfactant (Pluronic® L101; BASF, Ludwigshafen, Germany) and centrifuged at 200 × *g* for 5 min. The PDMS was aspirated away and replaced with PBS, followed by centrifugation to wash the microbeads and remove both residual PDMS and L101. This wash step was repeated three times. Formed microbeads were transferred to a clean centrifuge tube, resuspended in PBS and stored 4°C for subsequent analysis.

Quantification of microbead size

The effects of impeller speed and matrix composition on microbead size and size distribution were evaluated. The range of impeller speeds examined was 600, 750, 800, 1000, 1200 or 1400 rpm using the 25/75 microbead formulation. In addition, the ratio of chitosan to fibrin was varied as shown in Table 1. Collected microbeads were stained with neutralized EZBlue (Sigma), distributed in a clear dish and imaged under an inverted light microscope. Multiple digital images were taken of each preparation, and microbead diameter was measured on a random sample from each image using image analysis software (ImageJ, NIH) scaled using a calibrated microscopy reticle. Depending on the preparation, between 250 and 1800 microbeads were sized to produce histograms that provide both the average microbead size as well as a representation of the size distribution of the microbead population as a whole.

Visualization and quantification of protein in microbeads

The protein content of formed microbeads was visualized by staining with neutralized EZBlue reagent (Sigma). Neutralizing EZBlue with NaOH was necessary because acidic solutions dissolve chitosan and fibrin hydrogels. Equal volumes of microbead suspension and staining reagent were mixed and incubated for 24 h at room temperature. Stained microbeads were visualized and imaged under an inverted light microscope using phase contrast objectives.

Protein content in microbeads was quantified using a bicinchoninic acid protein assay kit (BCA; Thermo Pierce Inc., Rockford, IL). This assay causes fibrin to dissolve into solution, but leaves the non-protein chitosan matrix intact. BCA assay solution was added to microbead suspensions in 1:1 volume ratios and incubated at 37°C for 1 h. The absorbance of the microbead-BCA supernatant at 562 nm was read on a microplate reader (Multiskan® Spectrum; Thermo Fischer Scientific, Waltham, MA) and compared against a bovine serum albumin (BSA; Thermo Pierce Ltd) standard to determine the protein content of the sample. Protein concentration in the supernatant was converted to protein content of microbeads based on the total volume of microbeads, using the following equations:

$$[\text{microbeads}]=[\text{solution}]\times\frac{\text{solution vol.}}{\text{microbead vol.}}$$

$$\text{Microbead volume}=\sum_{\text{all microbeads in sample}}^{n}\frac{4}{3}\pi\left(\frac{d_i}{2}\right)^2$$

$$d_i=\text{diameter of individual microbead from microscopy and image analysis}$$

Cell culture and encapsulation in microbeads

Human neonatal dermal fibroblasts (hNDFb, Invitrogen, Carlsbad, CA) were cultured to passage 8 in complete medium consisting of Dulbecco's Modified Eagle Medium (DMEM; Mediatech, Manassas, VA) supplemented with 10% fetal bovine serum (Gibco® FBS; Invitrogen) and 1% penicillin/streptomycin/L-glutamine (Invitrogen). At the time of bead fabrication, hNDFb were counted using an automated cell counter (Coulter Multisizer) and 1.0×10^6 cells were suspended in the liquid matrix formulation at the desired chitosan/fibrinogen mass ratio. For microbead preparations containing cells, the fibrinogen was dissolved in culture medium containing 2.0 mg/mL aminocaproic acid (ACA, Sigma) to inhibit fibrin degradation by cell-secreted plasmin. Cell-containing microbead fabrication was performed using an impeller speed of 650 rpm in a sterile environment. Collected microbeads were resuspended and cultured in complete DMEM containing 2.0 mg/mL ACA. The dishes used to culture cell-containing microbeads were first coated with 0.5 mL of 2% autoclaved agarose (NuSieve; Lonza, Basel, Switzerland) to inhibit cell migration

outside of the microbeads. hNDFb encapsulated in microbeads were cultured for 8 days with medium changed every 2–3 days.

Cell viability and morphology in microbeads

Microbead samples were taken on day 1 and day 8 of culture for cell viability and morphology assessment. Microbeads were washed three times in PBS by centrifugation at 100 × *g* for 5 min. For cell viability assessment, a sample of washed microbeads was incubated for 1 h at 37°C with 4 μM calcein-AM and 4 μM ethidium homodimer (Live/Dead® Assay; Molecular Probes, Eugene, OR) in PBS. For morphology assessment, washed microbead samples were fixed in 1.5% paraformaldehyde (Electron Microscopy Sciences, Flatfield, PA) for 10 min and then washed three times, followed by incubation in 0.02% Triton X-100 (Sigma) for 15 min to permeabilize cell membranes. Microbeads were again washed three times and were then incubated for 1 h at 37°C in 4 μM ethidium homodimer and 0.16 μM Alexa Fluor® 488 phalloidin (Molecular Probes) in PBS. After incubation, all microbead samples were washed three times to remove residual stain. Fluorescence microscopy was performed on microbead samples using an inverted laser scanning confocal microscope (LSM-510, Carl Zeiss Microimaging, Thornwood, NY) with emission/excitation wavelengths of 488/530 nm for calcein, 488/630 nm for ethidium homodimer and 543/570 nm for phalloidin. Captured fluorescence microscopy images were merged and overlaid onto brightfield images of the microbead matrix using Matlab (MathWorks, Natick, MA) image processing algorithms.

Results and discussion

Control of microbead size and size distribution

Figure 2 shows histograms (Figures 2(a)—(f)) and average size data (Figures 2(g) and (h)) for chitosan–fibrin microbeads made under different conditions. In general, mean microbead diameter decreased with increasing impeller speed. Microbead populations exhibited approximately normal distributions, though the shape of the curve became progressively narrower as the impeller speed was increased (Figures 2(a)–(f)). The insets in Figures 2(a)—(f) show representative images of microbeads made at each condition. Figure 2(g) shows the average size and standard deviation of each microbead preparation. These data show an exponential trend towards lower microbead size. In addition, the standard deviation about the mean, which can be used as a measure of the dispersion of the size distribution (i.e. the variation in bead size), also followed a decreasing trend as impeller speed was increased. In these experiments, microbead size could be varied about sevenfold (280–40 μm) using impeller speeds from 600 to 1400 rpm. Varying the ratio of chitosan to fibrin in microbeads (Figure 2(h)) did not significantly affect the resulting average microbead diameter or size distribution of the microbead populations.

The fabrication method we used to create chitosan–fibrin microbeads relied on fluid shear forces to emulsify the hydrogel material. The resulting microbead size distribution was the result of a balance between surface tension and fluid shear forces exerted on the hydrogel droplets by the flowing PDMS fluid (Choi et al., 2007; Mark et al., 2009). Fluid shear force is a function of fluid velocity, which in our system was determined by impeller speed. Our findings confirmed that increasing impeller speed and fluid shear resulted in smaller microbeads, while there was no effect of changing the hydrogel composition. Other fabrication parameters that could affect microbead size include geometry of the impeller and emulsification vessel, as well as viscosity of the silicone oil, though these experimental conditions were not varied in this study.

Control of microbead size and size distribution is important for their use as cell delivery vehicles. The size of the microbeads dictates the lengths of the diffusion paths and rate of nutrient transport into the bead matrix. In addition, microbead size will affect the type of delivery method that can be used for therapeutic applications. Populations of very small beads can be handled as slurries and offer the possibility of minimally invasive delivery through standard needles. Our work has focused on microbeads in the 50–200 μm size range because such beads can hold multiple (tens to hundreds) of cells, and can be concentrated into injectable pastes (Batorsky et al., 2005; Lund et al., 2008). The size distribution of a microbead population (i.e. whether the microbeads are of uniform size, or whether a population contains beads in a large range of sizes) will determine the packing density and therefore the resulting overall porosity of a packed bed of microbeads. These parameters are critical in designing and evaluating microbeads for use in regenerative medicine.

Protein content in microbeads

Figure 3 shows the measured protein content of microbeads as a function of the amount of fibrinogen added to the hydrogel solution. It can be seen that at low levels of fibrinogen addition, the amount of protein in microbeads was approximately proportional to that in the starting material. However at higher levels (above about 50 wt.% fibrinogen), the amount of measured protein plateaued. Figure 4 shows optical microscopy images of chitosan–fibrin microbeads with the fibrin component stained blue. As expected, pure chitosan microbeads showed no staining (Figure 4(a)). In composite microbeads, there was clear phase separation between the chitosan and fibrin components (Figures 4(b)–(d)), with the chitosan forming a coat around the fibrin protein core. These images also reinforce the fact that fibrin content did not increase appreciably beyond the 50 wt.% level. The reason for the loss of fibrin from higher protein content formulations is not clear. However, it is possible that with larger amounts of fibrin, the polymerization process is not complete before the chitosan phase gels, resulting in loss of fibrin material.

The separation of phases in chitosan–fibrin microbeads may also be due to differences in the rate and/or mechanism of gel formation. Fibrin polymerization was initiated by addition of the enzyme thrombin, which cleaves the fibrinopeptide sequences from fibrinogen, resulting in spontaneous and rapid self assembly of the fibrin macromolecule (Mosesson, 2005). Gelation of the chitosan phase was caused by an increase in temperature and proton transfer from the β-glycerophosphate (Wang et al., 2010), which neutralizes the chitosan and causes gel formation. Thermosensitive chitosan gelation is a slower process than the enzymatic fibrin polymerization, and this may have caused the formation of separate phases. In addition, neutralization of the chitosan by β-glycerophosphate may have decreased the ionic interactions between phases, resulting in partitioning.

Cell viability and morphology in microbeads

Figure 5 shows vital staining of fibroblasts embedded in chitosan–fibrin microbeads of varying protein content. Laser scanning confocal microscopy was used to image fluorescently labelled fibroblasts in the interior of microbeads, and these images were then overlaid onto phase contrast images of the microbead matrix. Therefore, the cells observed in Figure 5 are embedded inside the 3D microbead matrix. The upper panels show cells 1 day after microbead fabrication, and demonstrate that cells can survive the emulsification and collection processes. In addition, these images suggest that cell retention in microbeads increased with increasing protein content, again plateauing above 50 wt.% fibrin. The lower panels show fibroblasts after 8 days of culture in microbeads. Viability remained high and there was evidence of cell proliferation in microbeads with higher fibrin content (50/50 and 25/75). In contrast, microbeads with lower fibrin content (100/0 and 75/25) contained more dead cells, and cell number did not increase over time. Chitosan has been shown to be

cytocompatible in previous studies using bulk gels, however it is a polysaccharide and does not contain the same abundance of cell binding sites as extracellular matrix proteins. It is not clear why cell viability and proliferation was reduced in the presence of increased chitosan content, however it may be related to the degree of cell adhesion or the mechanical properties of the material in microbead format. The preparations shown in Figure 5 contain considerable matrix debris due to the extensive amount of processing (multiple wash, incubation and centrifugation steps) required to perform the vital stain, which damages the microbeads. However, it should be noted that most microbead preparations stayed intact and were suitably robust for cell delivery (e.g. the microbeads in Figure 4 were processed less intensively and therefore their morphology is intact).

Figure 6 shows staining of the actin cytoskeleton and nucleus of cells embedded in microbeads for 1 day (top panels) and 8 days (middle and lower panels). Fibroblasts in microbeads containing more fibrin (50/50 and 25/75) were clearly more abundant and exhibited a more spread morphology than those in microbeads consisting predominantly of chitosan (100/0 and 75/25). Higher magnification images (lower panels) showed that cells in 50/50 and 75/25 microbeads also formed cell–cell contacts and interacted as clusters. Cell spreading is an indication of robust interaction with the extracellular matrix, and cell–cell contacts are important in controlling cell function. In this study, plasmin-mediated fibrin degradation was inhibited by the use of ACA in the culture medium, however over the longer term, the fibrin matrix could be degraded or remodelled through cellular action.

These results show that the presence of fibrin in the microbead matrix promoted increased cell retention during fabrication, as well as increased cell viability, spreading and proliferation in culture after fabrication. As expected from the protein incorporation data, there were no discernable differences between the higher fibrin formulations (50/50 and 25/75), presumably because the amount of fibrin plateaued. However, it was clear that fibrin incorporation improved the microbeads as cell delivery vehicles. The hNDFb used in this study generally stayed entrapped within the microbead matrix, though in some cases cells migrated to the surface of the microbeads. Cells do not bind strongly to chitosan alone because it is a marine-derived polysaccharide that lacks amino acid sequences for cell attachment. In contrast, fibrin is an extracellular matrix protein that is known to be conducive to cell growth (Rowe et al., 2007; Huang et al., 2010). Our results show that incorporation of fibrin into chitosan matrices can enhance cellular interactions with the matrix in microbeads, and thereby enhance their suitability for cell delivery.

Conclusions

We have developed a method to fabricate chitosan–fibrin microbeads using a facile water-in-oil emulsification process to embed living cells directly in the microbead matrix. The size and size distribution of such microbead preparations can be controlled by varying the process parameters, and we showed that increasing the impeller speed during fabrication results in smaller microbeads with a narrower size distribution. In these microbead formulations, chitosan provides structural integrity for the microbead, helping to maintain a spherical shape and to resist mechanical damage. Fibrin adds a bioactive protein component to the microbead matrix, allowing increased cellular interactions. The combination of these polymers results in a composite material that has improved properties, relative to either material alone.

Chitosan–fibrin microbeads prepared in this study had diameters ranging from 38 ± 10 μm to 275 ± 99 μm, depending on processing conditions. Fibrin was incorporated into the microbeads but there was clear phase separation between the chitosan and protein components due to the difference in gelling rates of the matrix components. In addition, the

degree of fibrin incorporation plateaued above approximately 50 wt.%. However, addition of fibrin clearly improved cell retention, viability, spreading, and proliferation in microbeads, presumably through enhanced cell–matrix and cell–cell interactions promoted by the presence of a natural extracellular matrix protein. Robust cell–matrix and cell–cell interactions are desirable in order to use these cues to guide cell function. Such biomacromolecule-based microbeads therefore have potential for cell delivery because their size and composition can be tailored to suit specific tissue regenerations applications.

Acknowledgments

This project was supported in part by the National Institute of Arthritis and Musculoskeletal and Skin Diseases through grant no. R01-AR053231.

References

Addo RT, Siddig A, Siwale R, Patel NJ, Akande J, Uddin AN, D'Souza MJ. Formulation, characterization and testing of tetracaine hydrochloride-loaded albumin-chitosan microparticles for ocular drug delivery. J Microencapsulation. 2010; 27:95–104. [PubMed: 20055748]

Ahmed TA, Dare EV, Hincke M. Fibrin: A versatile scaffold for tissue engineering applications. Tissue Eng Part B Rev. 2008; 14:199–215. [PubMed: 18544016]

Batorsky A, Liao J, Lund AW, Plopper GE, Stegemann JP. Encapsulation of adult human mesenchymal stem cells within collagen-agarose microenvironments. Biotechnol Bioeng. 2005; 92:492–500. [PubMed: 16080186]

Berger J, Reist M, Mayer JM, Felt O, Gurny R. Structure and interactions in chitosan hydrogels formed by complexation or aggregation for biomedical applications. Eur J Pharm Biopharm. 2004; 57:35–52. [PubMed: 14729079]

Breen A, O'brien T, Pandit A. Fibrin as a delivery system for therapeutic drugs and biomolecules. Tissue Eng Part B Rev. 2009; 15:201–14. [PubMed: 19249942]

Breslauer DN, Muller SJ, Lee LP. Generation of monodisperse silk micro-spheres prepared with microfluidics. Biomacromolecules. 2010; 11:643–7. [PubMed: 20131893]

Chan BP, Hui TY, Wong MY, Yip KH, Chan GC. Mesenchymal stem cell-encapsulated collagen microspheres for bone tissue engineering. Tissue Eng Part C Methods. 2010; 16:225–35. [PubMed: 20367213]

Chavakis E, Koyanagi M, Dimmeler S. Enhancing the outcome of cell therapy for cardiac repair: Progress from bench to bedside and back. Circulation. 2010; 121:325–35. [PubMed: 20083719]

Choi CH, Jung JH, Rhee YW, Kim DP, Shim SE, Lee CS. Generation of monodisperse alginate microbeads and in situ encapsulation of cell in microfluidic device. Biomed Microdevices. 2007; 9:855–62. [PubMed: 17578667]

Costa-Pinto AR, Correlo VM, Sol PC, Bhattacharya M, Charbord P, Delorme B, Reis RL, Neves NM. Osteogenic differentiation of human bone marrow mesenchymal stem cells seeded on melt based chitosan scaffolds for bone tissue engineering applications. Biomacromolecules. 2009; 10:2067–73. [PubMed: 19621927]

Cummings CL, Gawlitta D, Nerem RM, Stegemann JP. Properties of engineered vascular constructs made from collagen, fibrin, and collagen-fibrin mixtures. Biomaterials. 2004; 25:3699–706. [PubMed: 15020145]

Gorodetsky R, Clark RA, An J, Gailit J, Levdansky L, Vexler A, Berman E, Marx G. Fibrin microbeads (FMB) as biodegradable carriers for culturing cells and for accelerating wound healing. J Invest Dermatol. 1999; 112:866–72. [PubMed: 10383731]

Gorodetsky R, Vexler A, Levdansky L, Marx G. Fibrin microbeads (FMB) as biodegradable carriers for culturing cells and for accelerating wound healing. Methods Mol Biol. 2004; 238:11–24. [PubMed: 14970435]

Gurevich O, Vexler A, Marx G, Prigozhina T, Levdansky L, Slavin S, Shimeliovich I, Gorodetsky R. Fibrin microbeads for isolating and growing bone marrow-derived progenitor cells capable of forming bone tissue. Tissue Eng. 2002; 8:661–72. [PubMed: 12202005]

Hong H, Stegemann JP. 2D and 3D collagen and fibrin biopolymers promote specific ECM and integrin gene expression by vascular smooth muscle cells. J Biomater Sci Polym Ed. 2008; 19:1279–93. [PubMed: 18854122]

Huang NF, Chu J, Lee RJ, Li S. Biophysical and chemical effects of fibrin on mesenchymal stromal cell gene expression. Acta Biomater. 2010; 6:3947–56. [PubMed: 20678460]

Jiang T, Kumbar SG, Nair LS, Laurencin CT. Biologically active chitosan systems for tissue engineering and regenerative medicine. Curr Top Med Chem. 2008; 8:354–64. [PubMed: 18393897]

Kurita K. Chitin and chitosan: Functional biopolymers from marine crustaceans. J Mar Biotechnol (NY). 2006; 8:203–26.

Laurens N, Koolwijk P, De Maat MP. Fibrin structure and wound healing. J Thromb Haemost. 2006; 4:932–9. [PubMed: 16689737]

Lavertu M, Filion D, Buschmann MD. Heat-induced transfer of protons from chitosan to glycerol phosphate produces chitosan precipitation and gelation. Biomacromolecules. 2008; 9:640–50. [PubMed: 18186608]

Lee K, Chan CK, Patil N, Goodman SB. Cell therapy for bone regeneration – bench to bedside. J Biomed Mater Res B Appl Biomater. 2009; 89:252–63. [PubMed: 18777578]

Livoti CM, Morgan JR. Self-assembly and tissue fusion of toroid-shaped minimal building units. Tissue Eng Part A. 2010; 16:2051–61. [PubMed: 20109063]

Lund AW, Bush JA, Plopper GE, Stegemann JP. Osteogenic differentiation of mesenchymal stem cells in defined protein beads. J Biomed Mater Res B Appl Biomater. 2008; 87:213–21. [PubMed: 18431753]

Lund AW, Yener B, Stegemann JP, Plopper GE. The natural and engineered 3D microenvironment as a regulatory cue during stem cell fate determination. Tissue Eng Part B Rev. 2009; 15:371–80. [PubMed: 19505193]

Madihally SV, Matthew HW. Porous chitosan scaffolds for tissue engineering. Biomaterials. 1999; 20:1133–42. [PubMed: 10382829]

Maeng YJ, Choi SW, Kim HO, Kim JH. Culture of human mesenchymal stem cells using electrosprayed porous chitosan microbeads. J Biomed Mater Res A. 2010; 92:869–76. [PubMed: 19280627]

Mark D, Haeberle S, Zengerle R, Ducree J, Vladisavljevic GT. Manufacture of chitosan microbeads using centrifugally driven flow of gel-forming solutions through a polymeric micronozzle. J Colloid Interface Sci. 2009; 336:634–41. [PubMed: 19428020]

Mazumder MA, Burke NA, Shen F, Potter MA, Stover HD. Core-cross-linked alginate microcapsules for cell encapsulation. Biomacromolecules. 2009; 10:1365–73. [PubMed: 19397289]

Mcguigan AP, Bruzewicz DA, Glavan A, Butte MJ, Whitesides GM. Cell encapsulation in sub-mm sized gel modules using replica molding. PLoS One. 2008; 3:e2258. [PubMed: 18493609]

Mosesson MW. Fibrinogen and fibrin structure and functions. J Thromb Haemost. 2005; 3:1894–904. [PubMed: 16102057]

Nair LS, Starnes T, Ko JW, Laurencin CT. Development of injectable thermogelling chitosan-inorganic phosphate solutions for biomedical applications. Biomacromolecules. 2007; 8:3779–85. [PubMed: 17994699]

Natesan S, Baer DG, Walters TJ, Babu M, Christy RJ. Adipose-derived stem cell delivery into collagen gels using chitosan microspheres. Tissue Eng Part A. 2010; 16:1369–84. [PubMed: 19916819]

Nichol JW, Khademhosseini A. Modular tissue engineering: Engineering biological tissues from the bottom up. Soft Matter. 2009; 5:1312–9. [PubMed: 20179781]

Perka C, Arnold U, Spitzer RS, Lindenhayn K. The use of fibrin beads for tissue engineering and subsequential transplantation. Tissue Eng. 2001; 7:359–61. [PubMed: 11429155]

Rowe SL, Lee S, Stegemann JP. Influence of thrombin concentration on the mechanical and morphological properties of cell-seeded fibrin hydrogels. Acta Biomater. 2007; 3:59–67. [PubMed: 17085089]

Sakai S, Kawabata K, Ono T, Ijima H, Kawakami K. Development of mammalian cell-enclosing subsieve-size agarose capsules (<100 micron) for cell therapy. Biomaterials. 2005; 26:4786–92. [PubMed: 15763258]

Solorio L, Zwolinski C, Lund AW, Farrell MJ, Stegemann JP. Gelatin micro-spheres crosslinked with genipin for local delivery of growth factors. J Tissue Eng Regen Med. 2010; 4:514–23. [PubMed: 20872738]

Wang L, Stegemann JP. Thermogelling chitosan and collagen composite hydrogels initiated with beta-glycerophosphate for bone tissue engineering. Biomaterials. 2010; 31:3976–85. [PubMed: 20170955]

Yamaguchi I, Itoh S, Suzuki M, Sakane M, Osaka A, Tanaka J. The chitosan prepared from crab tendon I: The characterization and the mechanical properties. Biomaterials. 2003; 24:2031–6. [PubMed: 12628822]

Yu J, Du KT, Fang Q, Gu Y, Mihardja SS, Sievers RE, Wu JC, Lee RJ. The use of human mesenchymal stem cells encapsulated in RGD modified alginate microspheres in the repair of myocardial infarction in the rat. Biomaterials. 2010; 31:7012–20. [PubMed: 20566215]

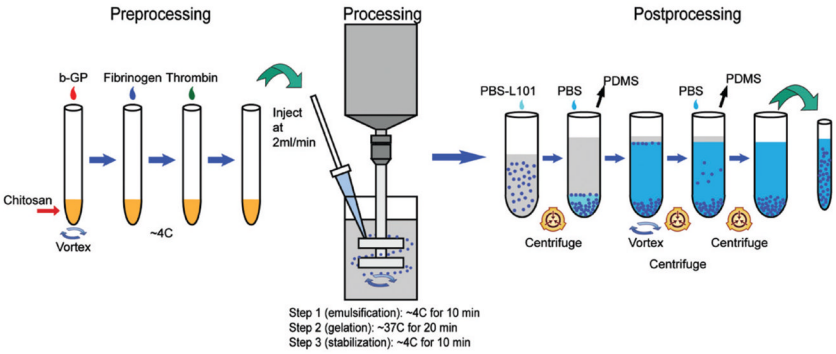

Figure 1.
Schematic of microbead fabrication process showing main preprocessing, fabrication and post-processing steps and solutions.

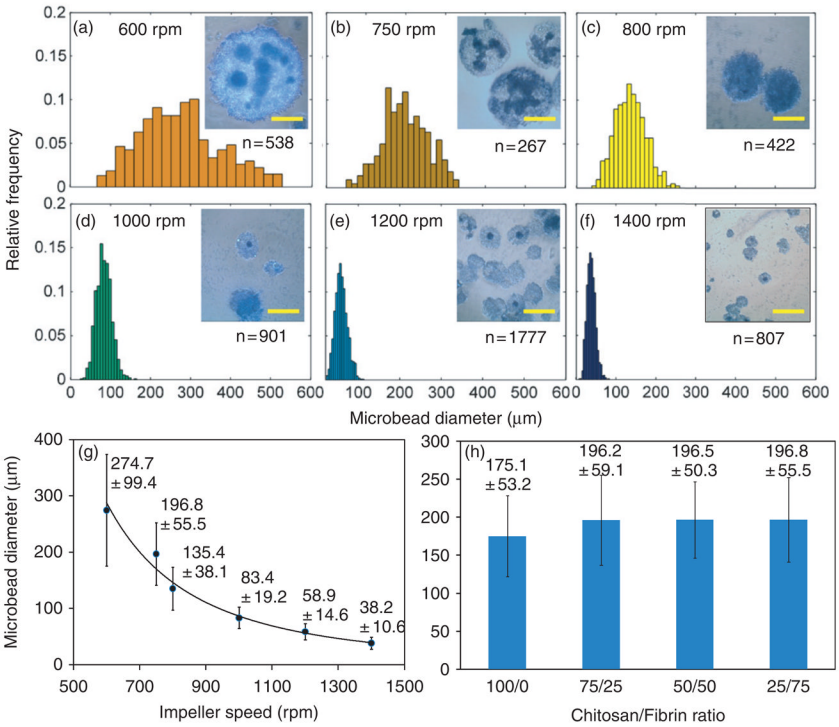

Figure 2.

(a–f) Effect of impeller speed on 25/75 CHI/FIB microbead diameter. Inset shows phase contrast images of microbeads with fibrin component stained blue (scale bar represents 100 μm). (g) Average and standard deviation of microbead diameter as a function of impeller speed. (h) Effect of microbead composition on microbead diameter at 750 rpm impeller speed. N = 3–4 for all data.

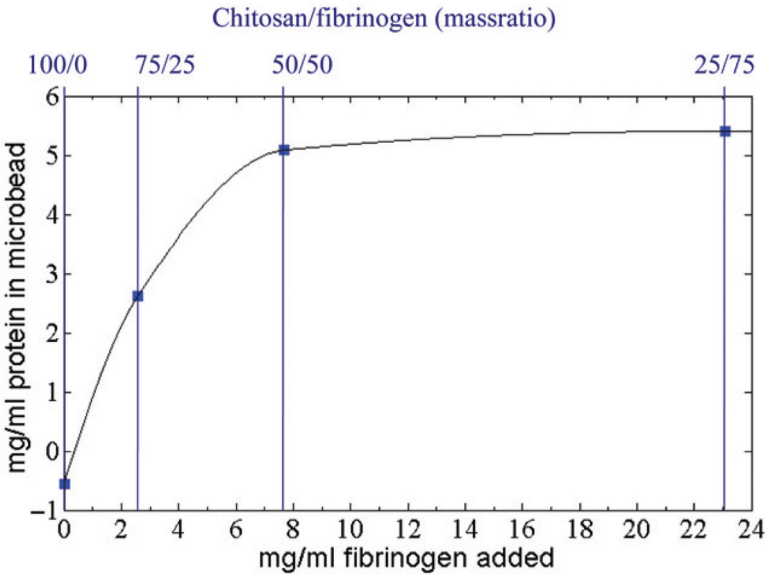

Figure 3.

Final protein content of microbeads as a function of amount of fibrinogen added to the initial matrix solution.

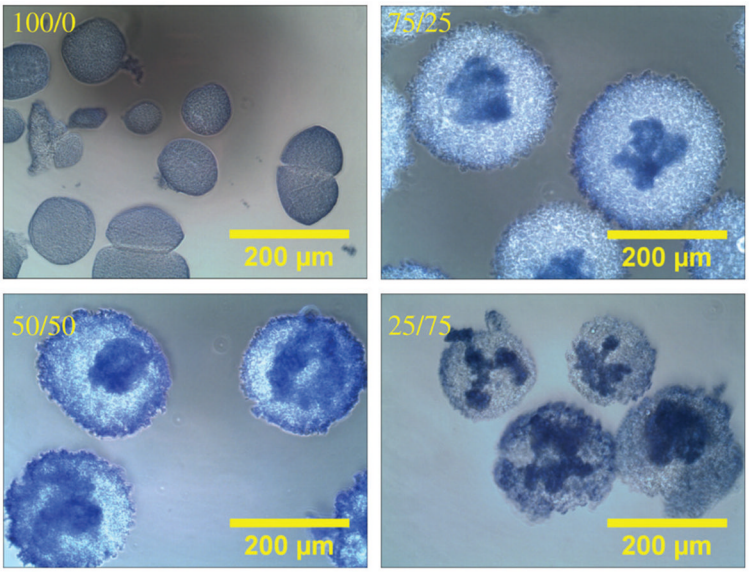

Figure 4.
Phase contrast images of microbeads made with varying CHI/FIB ratios. Fibrin has been stained blue.

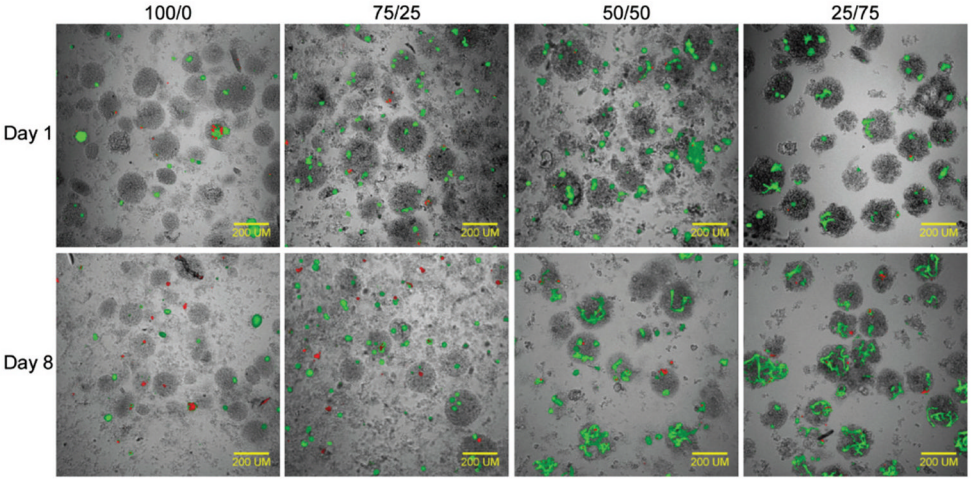

Figure 5.

Viability staining of fibroblasts embedded inside chitosan–fibrin microbeads with varying CHI/FIB ratios at day 1 and day 8 post-fabrication. The cytoplasm of living cells is stained green and the nucleus of dead cells is stained red. Scale bars represent 200 μm.

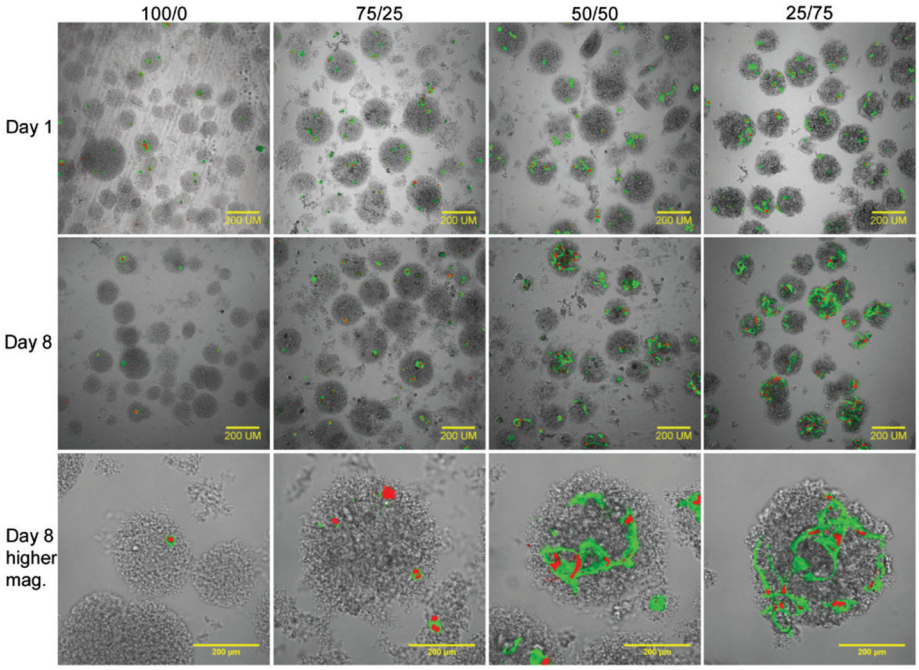

Figure 6.

Morphological staining of fibroblasts embedded inside chitosan–fibrin microbeads with varying CHI/FIB ratios at day 1 and day 8 post-fabrication. The actin cytoskeleton is stained green and the nucleus is stained red. Scale bars represent 200 μm.

Table 1

Amount of fibrinogen in chitosan/fibrin microbeads.

CHI/FIB ratio (mg/mg)	FIB added (mg/mL)
100/0	0
75/25	2.56
50/75	7.69
25/75	23.1